

Brain-PET modelling in clinical studies



Marco Bucci, PhD, Docent
Turku PET Centre and Karolinska Institutet



Outline

- Modelling (methods)
 - Kinetic modelling vs Statistical modelling
 - From visual to quantitation
 - Input function modelling
- Brain FDG in research and clinic
 - Metabolic field – Obesity and Diabetes
- Amyloid PET in dementia research and tertiary memory clinic
 - VR vs SUVR
- Tau PET (and Amyloid PET) in research and tertiary memory clinic
 - ATN paper – metaROI and LMM
 - VR and Plasma Biomarkers and LASSO
 - SuStaln
 - ML Clustering

Modelling methods in Brain PET imaging: Kinetic vs Statistical models

Kinetic models

- designed to describe and quantify the underlying biological processes that govern the behaviour of the radiotracer within the brain.
- based on physiological and biochemical principles and involve the estimation of parameters related to these processes.
- Examples: Compartmental models, Receptor Binding models, Graphical Models, Spectral Analysis

Statistical models

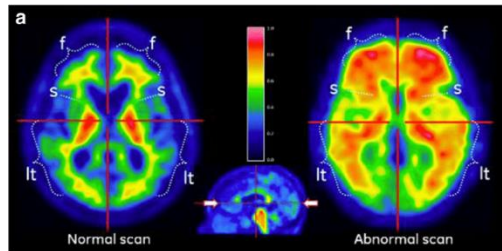
- focused on the statistical properties of the PET signal, often using data-driven approaches to analyze or interpret the imaging data.
- they may not directly describe the underlying biological processes but are useful for extracting patterns, trends, and significant differences in the data.
- Examples: Statistical Parametric Mapping (Atlas ROIs or Clusters), Machine Learning (ML) models (supervised, unsupervised, deep learning, LASSO), Bayesian models

Modelling methods in Brain PET imaging

Modelling: the process of creating mathematical or computational representations that describe and quantify the underlying biological, physiological, or biochemical processes that govern the distribution, kinetics, and interaction of a radiotracer within the brain.



Visual reading

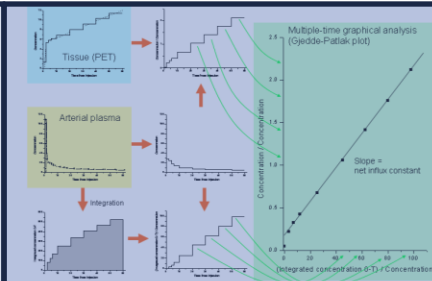


(Non-compart.) Semi-quantitative methods

$$SUV = \frac{[\text{radioph.}] (\text{kBq/mL})}{\text{injected activity (MBq)}} \cdot \text{normalizing fct (BW, BSA, LBM, ...)}$$

$$SUVR = \frac{SUV_{\text{Target region (brain ROI)}}}{SUV_{\text{Reference region (brain ROI)}}$$

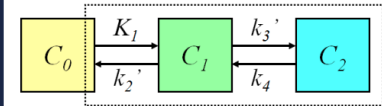
Input-function indep.



Input-function dep.



Fully quantitative methods



Dynamic PET and Input-function dep.

Input recovery method: improve quality of sampled input functions



metabolites



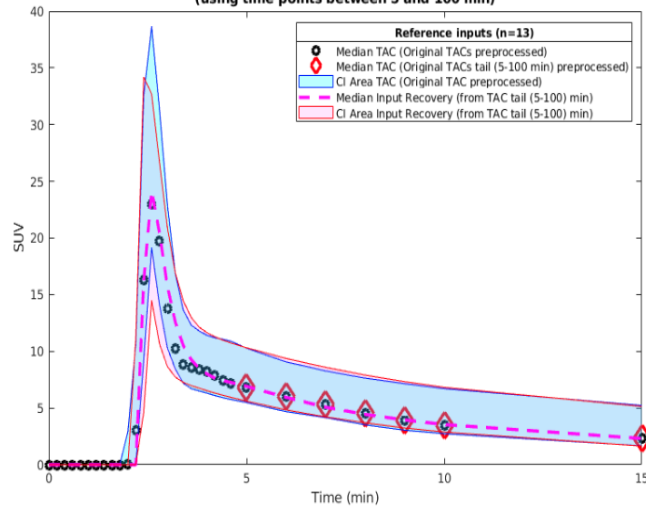
Article

Kinetic Modelling of Brain [^{18}F]FDG PET time activity curves with Input Function Recovery (IR) method

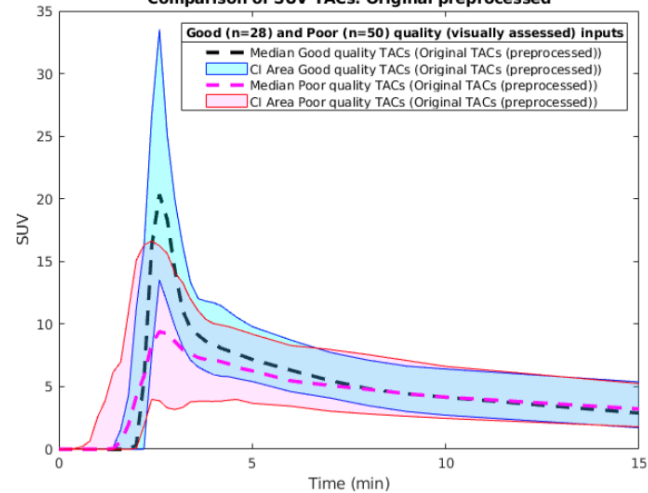
Marco Bucci ^{1,2,3,4,5,*}, Eleni Rebelos ², Vesa Oikonen ², Juha Rinne ¹, Lauri Nummenmaa ^{2,6}, Patricia Iozzo ⁷ and Pirjo Nuutila ^{2,8}

Validation of IR method

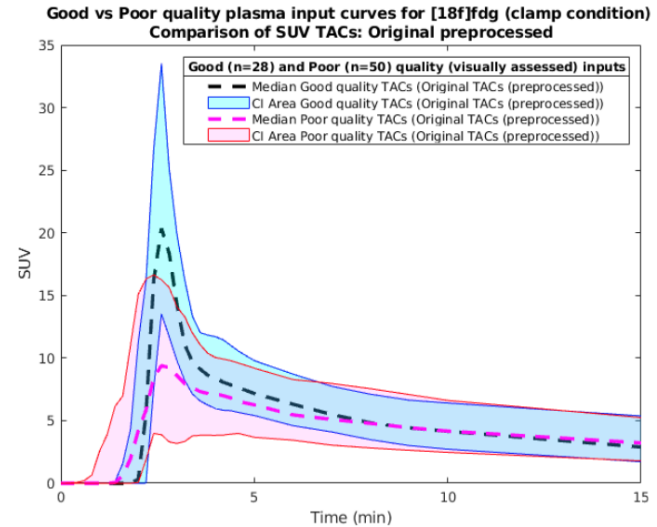
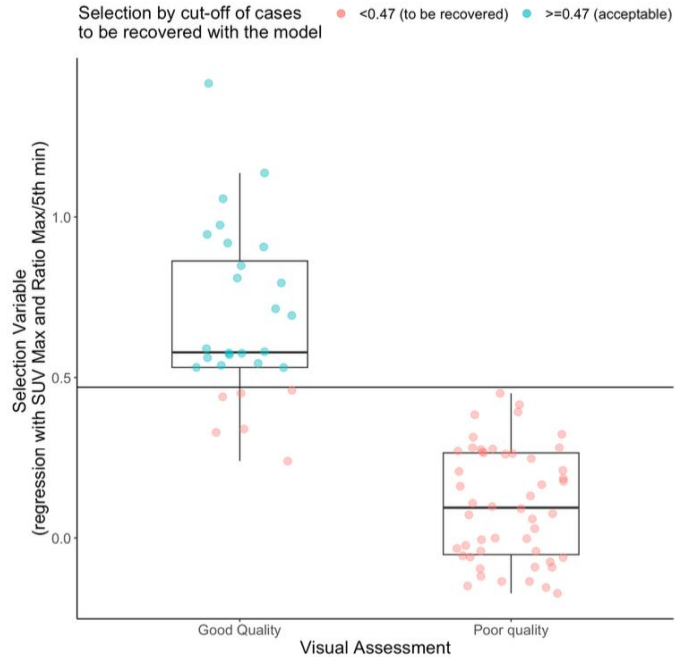
Comparison of SUV TACs: Original preprocessed (PALZ) vs Recovered Input with Feng/Bayesian fit (using time points between 5 and 100 min)



Good vs Poor quality plasma input curves for [18f]fdg (clamp condition)
Comparison of SUV TACs: Original preprocessed



Validation of IR method



Validation of IR method

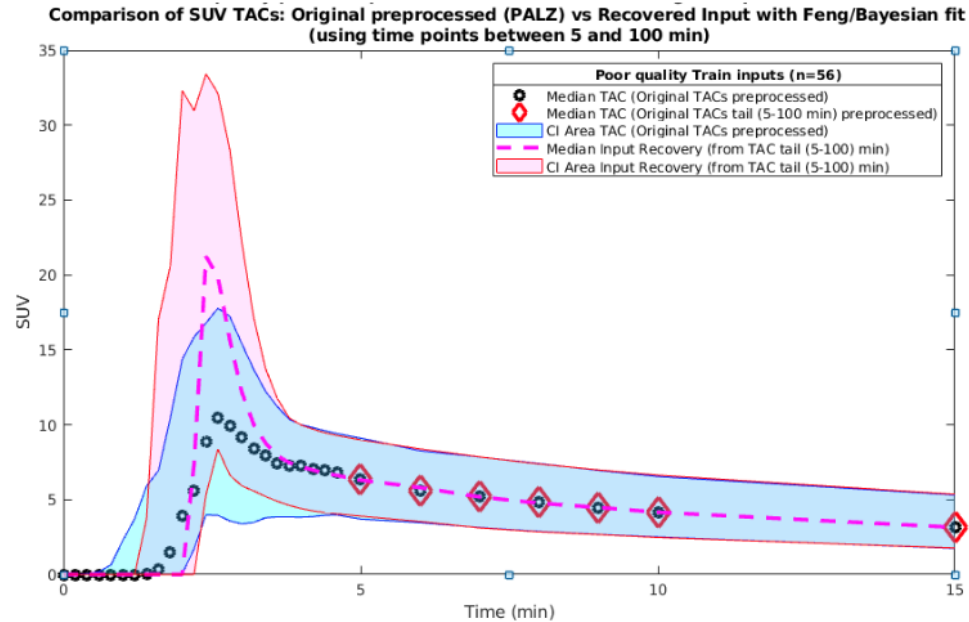
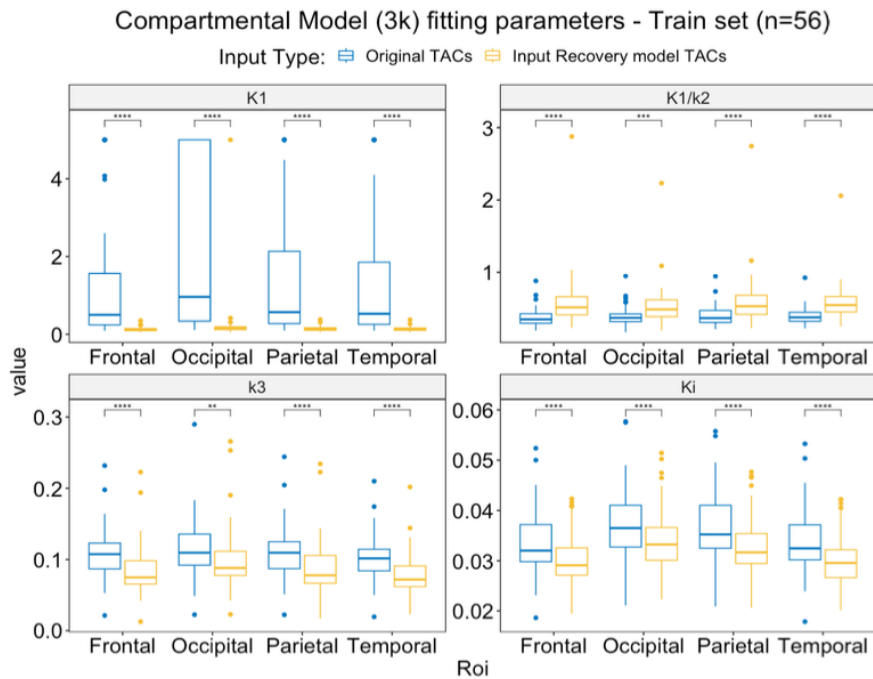
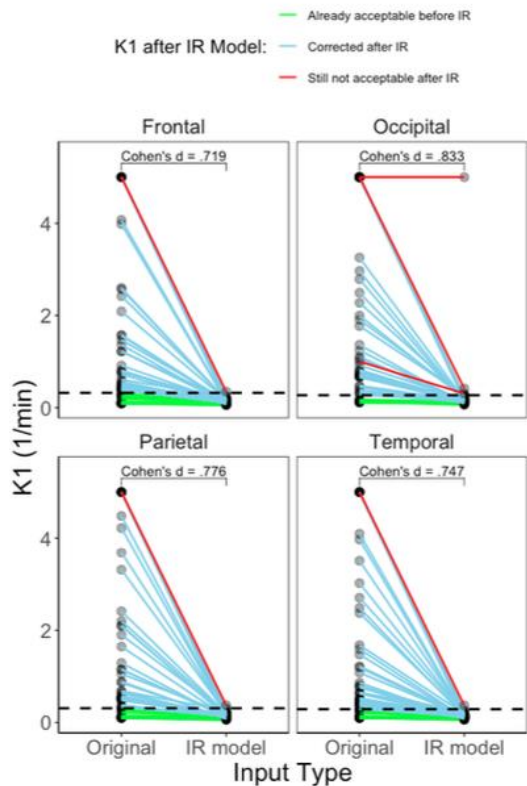


Figure 6. Poor-quality Input TACs (Train set, n = 56) – Original and Recovered by the Feng-Bayes model. The peak is recovered while the tail is kept similar to the original curves.

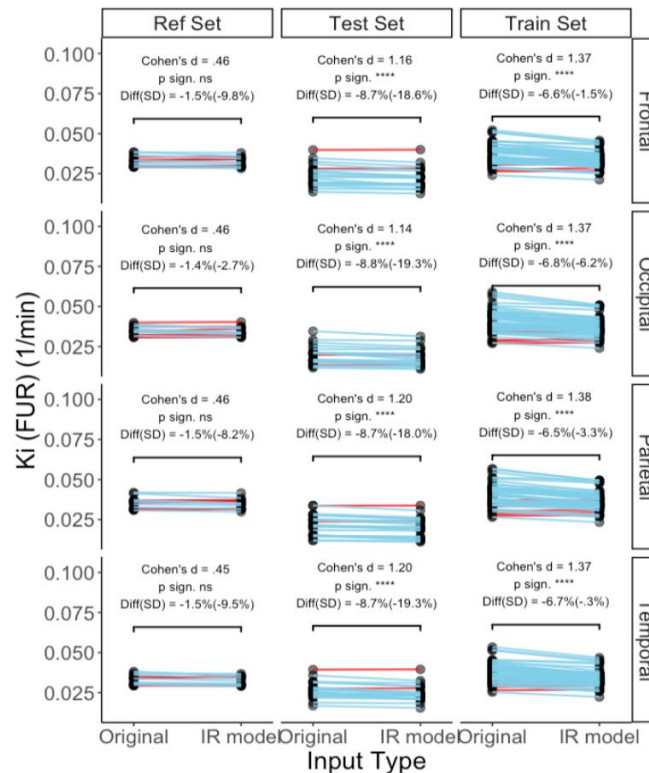
Results (1) from IR method applied to the train set



Results (2): K1 of train set and FUR of all sets



Bucci et al. Metabolites 2024



Methods in Brain PET imaging: Input modelling conclusions

- Input function quality affects modelling parameters and should be corrected when possible
- Input recovery from samples of the tail of the time activity curve in the plasma is a feasible method of correction
- There are also different ways to derive input from image but good quality images (not suitable for old scans) and arteries should be in the Field Of View. (not shown)



Brain PET: FDG

Brain FDG: Example of Metabolic Study

Insulin Resistance Is Associated With Enhanced Brain Glucose Uptake During Euglycemic Hyperinsulinemia: A Large-Scale PET Cohort

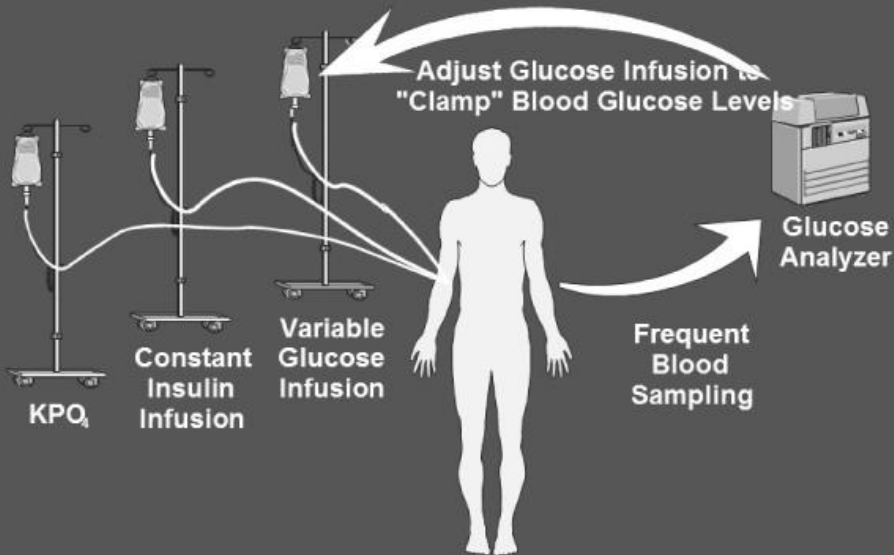
*Eleni Rebelos,¹ Marco Bucci,¹
Tomi Karjalainen,¹ Vesa Oikonen,¹
Alessandra Bertoldo,²
Jarna C. Hannukainen,¹ Kirsi A. Virtanen,^{1,3}
Aino Latva-Rasku,¹ Jussi Hirvonen,⁴
Ilkka Heinonen,^{1,5} Riitta Parkkola,⁴
Markku Laakso,⁶ Ele Ferrannini,⁷
Patricia Iozzo,^{1,7} Lauri Nummenmaa,^{1,8} and
Pirjo Nuutila^{1,9}*

Diabetes Care 2021;44:788–794 | <https://doi.org/10.2337/dc20-1549>

- Type of modelling: semiquantitative (BGU, brain glucose uptake (graphical analysis (FUR, fractional uptake rate))
- Type of statistical inference: Bayesian

HYPERINSULINEMIC EUGLYCEMIC GLUCOSE CLAMP TECHNIQUE
TO MEASURE THE WHOLE BODY GLUCOSE DISPOSAL DURING INSULIN STIMULATION

Hyperinsulinemic Euglycemic Glucose Clamp



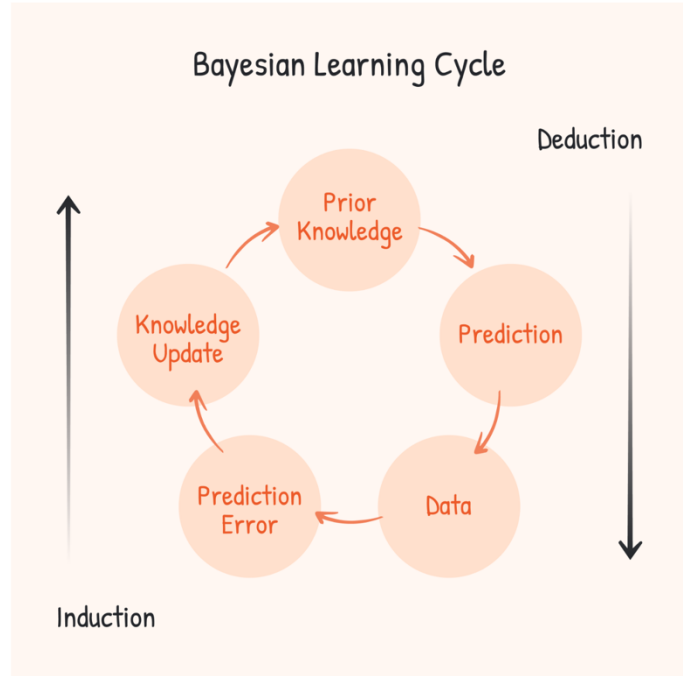
At "Steady-State", Glucose Infusion = Net Glucose Utilization

The **m-value** (or **glucose infusion rate, GIR**) represents the amount of glucose that needs to be infused per minute to maintain a constant euglycemic state (normal blood glucose level) during a hyperinsulinemic-euglycemic clamp study. The higher the m-value, the more insulin-sensitive the subject is, as it indicates that more glucose needs to be infused to maintain blood glucose levels in the presence of high insulin.

Statistical inferences: Bayesian vs frequentist

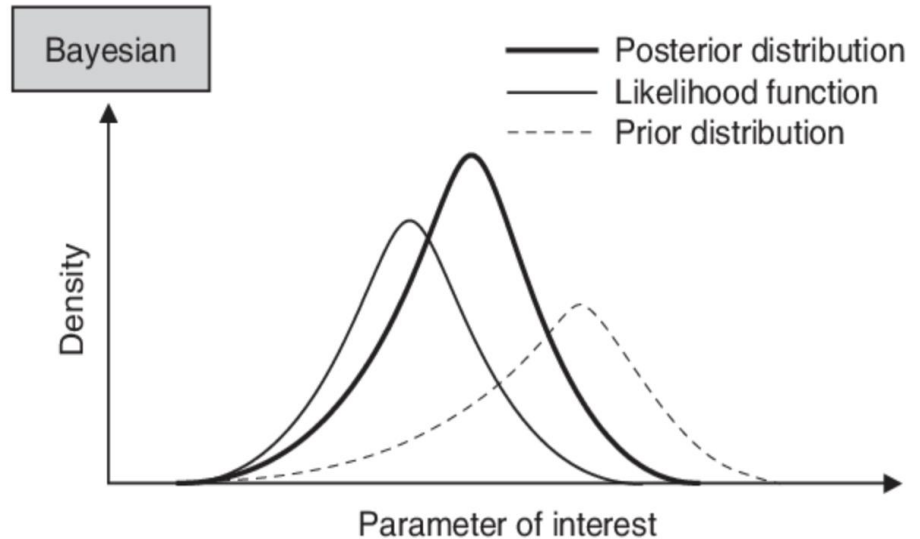
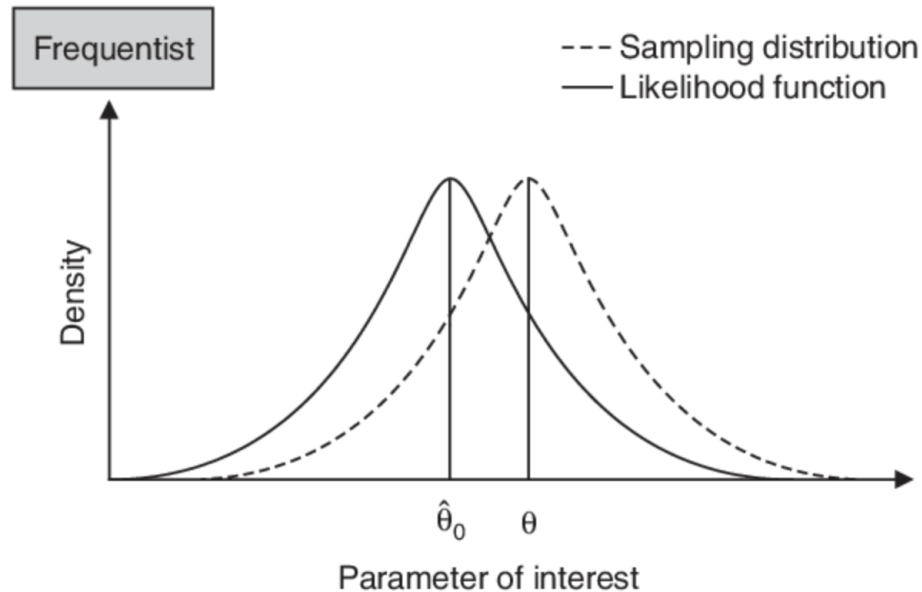
- Bayesian modelling

Bayesian vs. Frequentist Summary



| Attributes: | Bayesian: | Frequentist: |
|-------------------------------|---|---|
| What is it? | Probability distribution around the parameters | Parameters are fixed and a single point |
| What does it question? | Given the data, what is the probability of the hypothesis? | Is the hypothesis true or false? |
| What does it require? | Prior knowledge/information and any dataset. | A stopping criterion |
| What does it output? | A for or against probability about the hypothesis. | point estimate (p-value) |
| Main advantage | Backed up with evidence and can apply new information | They are simple and easy to use, and does not need prior knowledge |
| Main disadvantage | Requires advanced statistics | Highly dependent on the sample size, and only give a yes or no output |
| When should I use it? | Limited your data when you have priors Uses more computing power | With a large amount of data |

Statistical inferences: Bayesian vs frequentist



Source: Skrepnek, G.H. (2007) *Pharmacoconomics*, 25(8): 649-64

Brain FDG: Posterior distributions predicting BGU

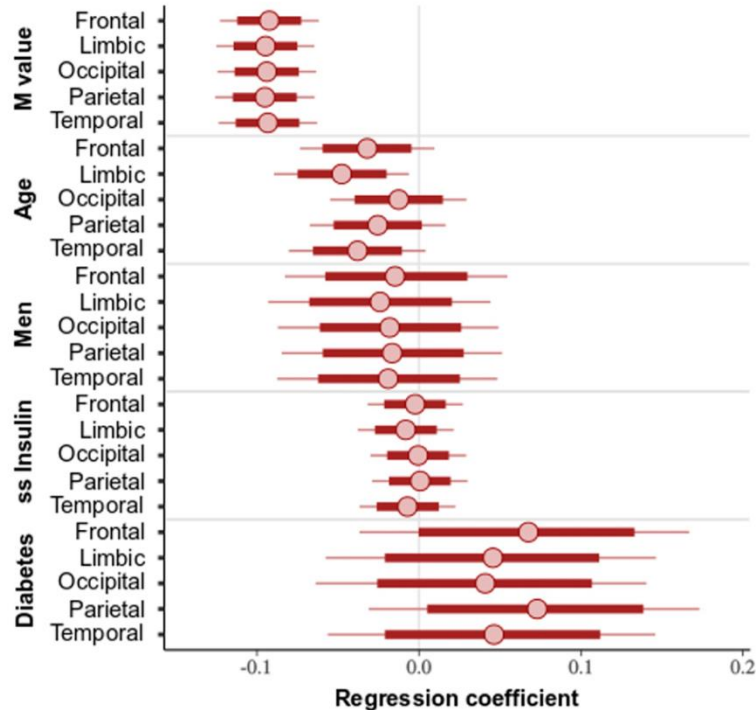


Figure 2—Posterior intervals of the regression coefficients for the variables of interest predicting BGU. The thick lines represent the 80% posterior intervals, the thin lines represent the 95% posterior intervals, and the circles represent posterior means. ss, steady state.

Table 1—Anthropometric and biochemical characteristics of the study participants

| | Men (<i>n</i> = 63) | | | Women (<i>n</i> = 131) | | |
|---|----------------------|------|-----------|-------------------------|------|------------|
| | Mean | SD | Range | Mean | SD | Range |
| Age (years) | 56 | 11 | 20–69 | 56 | 14 | 23–80 |
| BMI ($\text{kg} \cdot \text{m}^{-2}$) | 29 | 6 | 22–48 | 30 | 7 | 19–51 |
| HbA _{1c} | | | | | | |
| % | 5.6 | 0.3 | 5.1–6.3 | 5.6 | 0.4 | 4.9–7.1 |
| mmol/mol | 38 | 4 | 32–45 | 38 | 8 | 30–54 |
| M value ($\mu\text{mol} \cdot \text{kg}_{\text{FFM}}^{-1} \cdot \text{min}^{-1}$) | 40.2 | 24.5 | 7.9–130.8 | 49.1 | 25.3 | 10.3–138.2 |
| Type 2 diabetes, <i>n</i> (%) | 7 (11) | | | 20 (15) | | |

The **m-value** (or **glucose infusion rate, GIR**) represents the amount of glucose that needs to be infused per minute to maintain a constant euglycemic state (normal blood glucose level) during a hyperinsulinemic-euglycemic clamp study. The higher the m-value, the more insulin-sensitive the subject is, as it indicates that more glucose needs to be infused to maintain blood glucose levels in the presence of high insulin.

Brain FDG: Posterior distributions predicting BGU

Higher BGU is associated with lower M-Value (insulin resistance) probably due to increased brain inflammation

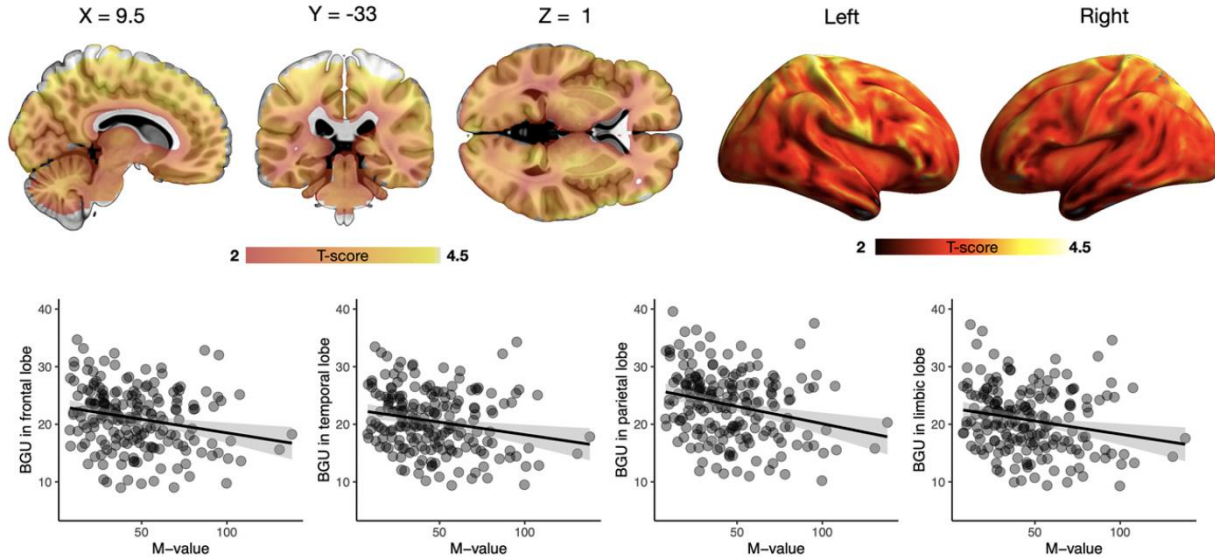


Figure 3—Brain clusters (as defined by false discovery rate–corrected statistical parametric mapping one-sample t test) for the association between BGU during clamp and M value and the corresponding scatterplots.

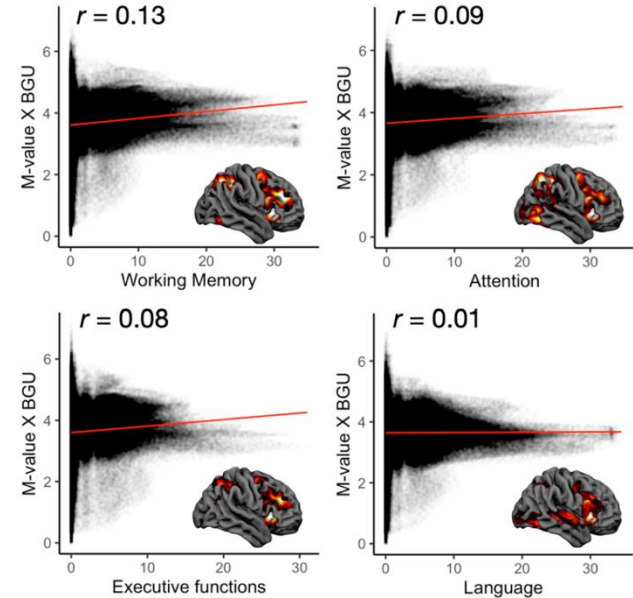


Figure 4—Spatial correlation between the regional M-value–dependent insulin-stimulated BGU (y-axis) and meta-analytic blood oxygenation level–dependent functional MRI activation patterns for four basic cognitive functions retrieved from the Neurosynth database (<https://www.neurosynth.org>). These results show how well the M value–dependent BGU effects correspond with cerebral localization of different cognitive functions.



Brain PET: Amyloid (Flutemetamol)

Pathological mechanisms involved in AD

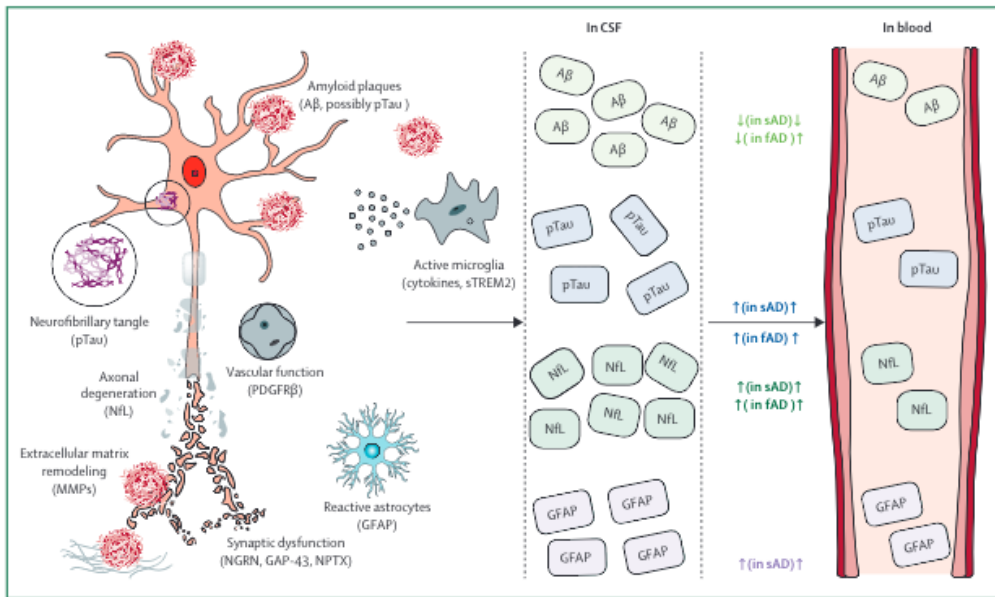
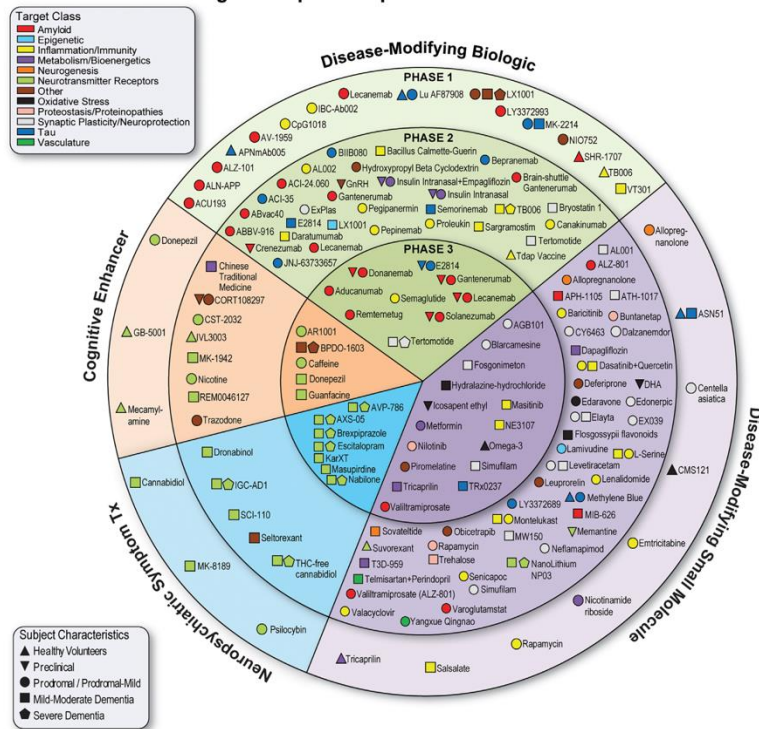


Figure 1: Pathological mechanisms involved in Alzheimer's disease and their associated biofluid-based biomarkers
 Alzheimer's disease has a complex pathophysiology. Biofluid-based biomarkers that can be reliably measured in both blood and CSF are: Aβ, pTau, NFL, and GFAP. Biomarkers with strong potential in CSF only include: cytokines, sTREM2, PDGFRβ, MMPs, NGRN, GAP-43, and NPTX. Aβ=amyloid β. NFL=neurofilament light chain. pTau=phosphorylated tau. GFAP=glial fibrillary acidic protein. MMP=matrix metalloproteinase. sAD=sporadic Alzheimer's disease. fAD=familial Alzheimer's disease.

2023 Alzheimer's Drug Development Pipeline



Brain Amyloid PET: VR vs SUVR discordance

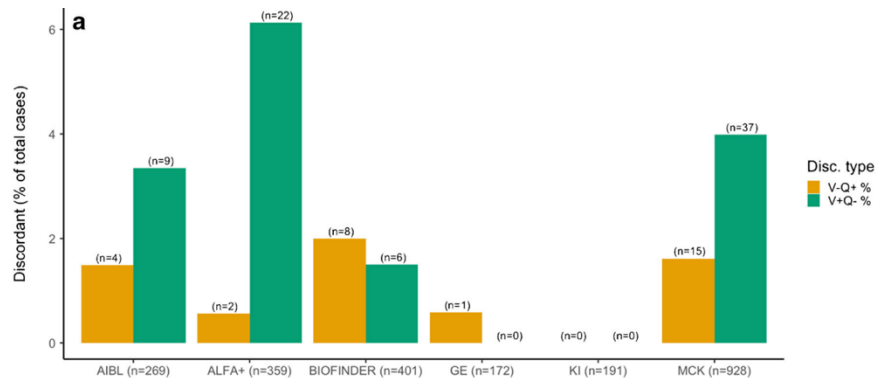
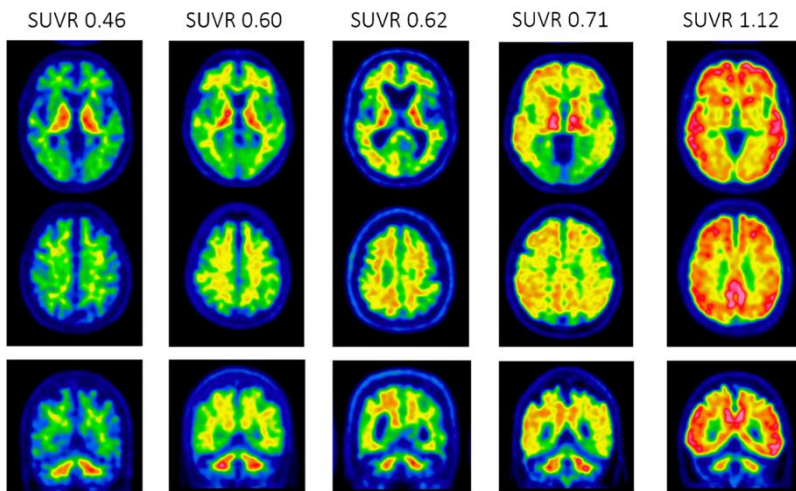
European Journal of Nuclear Medicine and Molecular Imaging (2021) 48:2183–2199
<https://doi.org/10.1007/s00259-021-05311-5>

ORIGINAL ARTICLE



A multisite analysis of the concordance between visual image interpretation and quantitative analysis of [¹⁸F]flutemetamol amyloid PET images

Marco Bucci¹ · Irina Savitcheva² · Gill Farrar³ · Gemma Salvadó^{4,5} · Lyduine Collij⁶ · Vincent Doré^{7,8} · Juan Domingo Gisbert^{4,5,9,10} · Roger Gunn^{11,12} · Bernard Hanseeuw^{13,14} · Oskar Hansson¹⁵ · Mahnaz Shekari^{4,5,9} · Renaud Lhommelet¹³ · José Luis Molinuevo^{4,5,9,16} · Christopher Rowe^{7,17} · Cyrille Sur¹⁸ · Alex Whittington¹¹ · Christopher Buckley³ · Agneta Nordberg^{1,19}



| | V+Q- (n=37) | V-Q+ (n=14) | Total (n=51) | p value |
|------------------|----------------|----------------|-----------------|--------------|
| Diagnosis | | | | 0.014 |
| HC | 7 (50 %) | 7 (50 %) | 14 | |
| HC(ADO) | 22 (91.7 %) | 2 (8.3 %) | 24 | |
| SCD | 2 (40 %) | 3 (60 %) | 5 | |
| MCI | 4 (66.7 %) | 2 (33.3 %) | 6 | |
| AD | 1 (100 %) | 0 (0 %) | 1 | |
| nonAD | 1 (100 %) | 0 (0 %) | 1 | |

Brain Amyloid PET: VR vs SUVR paper discordance: sensitivity analysis

European Journal of Nuclear Medicine and Molecular Imaging (2021) 48:2183–2199
<https://doi.org/10.1007/s00259-021-05311-5>

ORIGINAL ARTICLE



A multisite analysis of the concordance between visual image interpretation and quantitative analysis of [¹⁸F]flutemetamol amyloid PET images

Marco Bucci¹ · Irina Savitcheva² · Gill Farrar³ · Gemma Salvadó^{4,5} · Lyduine Collij⁶ · Vincent Doré^{7,8} · Juan Domingo Gispert^{4,5,9,10} · Roger Gunn^{11,12} · Bernard Hanseeuw^{13,14} · Oskar Hansson¹⁵ · Mahnaz Shekar^{4,5,9} · Renaud Lhommeil¹⁵ · José Luis Molinuevo^{4,5,9,16} · Christopher Rowe^{7,17} · Cyrille Sur¹⁸ · Alex Whittington¹¹ · Christopher Buckley¹ · Agneta Nordberg^{1,19}

Different sites, maybe necessary harmonization (ComBat) or CL scaling

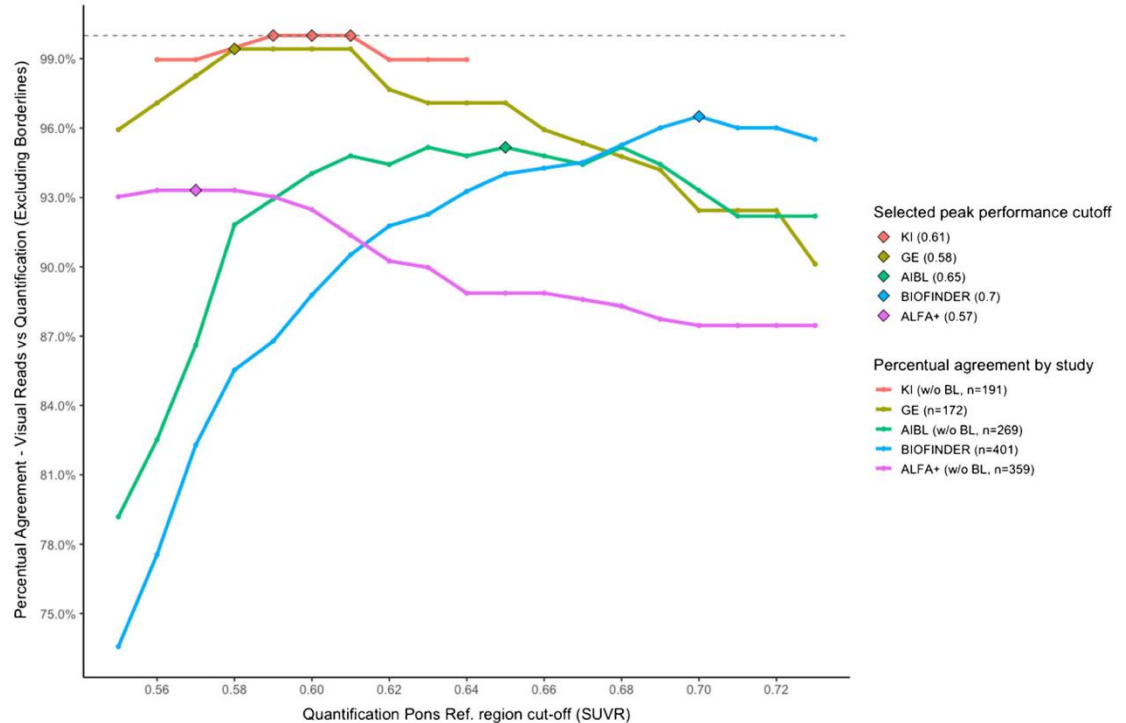


Fig. 1 Change in % agreement between visual and quantitative image interpretation around the SUVR pons threshold of 0.55 to 0.74 (with borderlines (BL) excluded). Note: The number of BL cases excluded is 21, 2 and 7 for KAROLINSKA, ALFA+ and AIBL, respectively

Brain Amyloid PET: VR vs SUVR paper discordance: sensitivity analysis

| | V-Q+ (N=21) | V+Q- (N=4) | Total (N=25) | p value |
|--|-------------|------------|--------------|---------|
| Progression to any clinical diagnosis | | | | 0.524 |
| Clinical progression | 14 (66.7%) | 2 (50.0%) | 16 (64.0%) | |
| stable | 7 (33.3%) | 2 (50.0%) | 9 (36.0%) | |
| Progression to AD/Other Diagnosis | | | | 0.322 |
| Progression to AD | 8 (38.1%) | 0 (0.0%) | 8 (32.0%) | |
| Progression to Other Diagnosis | 6 (28.6%) | 2 (50.0%) | 8 (32.0%) | |
| stable | 7 (33.3%) | 2 (50.0%) | 9 (36.0%) | |
| Progression in detail | | | | 0.206 |
| HC to SCD | 1 (4.8%) | 1 (25.0%) | 2 (8.0%) | |
| MCI to AD | 4 (19.0%) | 0 (0.0%) | 4 (16.0%) | |
| MCI to Parkinsonian | 2 (9.5%) | 0 (0.0%) | 2 (8.0%) | |
| SCD to AD | 4 (19.0%) | 0 (0.0%) | 4 (16.0%) | |
| SCD to MCI | 0 (0.0%) | 1 (25.0%) | 1 (4.0%) | |
| SCD to Parkinsonian | 1 (4.8%) | 0 (0.0%) | 1 (4.0%) | |
| SCD to Vascular | 2 (9.5%) | 0 (0.0%) | 2 (8.0%) | |
| stable | 7 (33.3%) | 2 (50.0%) | 9 (36.0%) | |

- Performing **Competing Risk Regression** analysis that took advantage of the full follow-up data (up to 7 years), using censoring similar to a survival analysis and discounting the contribution of the competing events (AD and OD progression):
- the **V-Q+ discordant cases were 11% (CI 95%: 4%-34%) more likely to progress to AD than V+Q- discordant cases (p<0.001).**



Brain PET: Amyloid (Flutemetamol) + Tau (Fluortaucipir)

AD biomarkers: the AT(N) framework

- Some of the AD biomarkers are designed to target AD-specific changes, such as the deposition of amyloid- β (A) and tau (T), while others the downstream neurodegeneration (N).
- The AT(N) framework from Jack et al (2018):
 - ❖ A - Amyloid- β (PET or CSF)
 - ❖ T – Tau (PET or CSF p-tau)
 - ❖ (N) – Neurodegeneration (MRI, CSF t-tau, FDG PET)
- Note that in the original formulation the biomarkers in the same category (A,T or N) can be used indistinctively!



ATN paper: aims

- a) to assess the agreement/concordance of the imaging and CSF biomarkers across the ATN components and as ATN profiles;

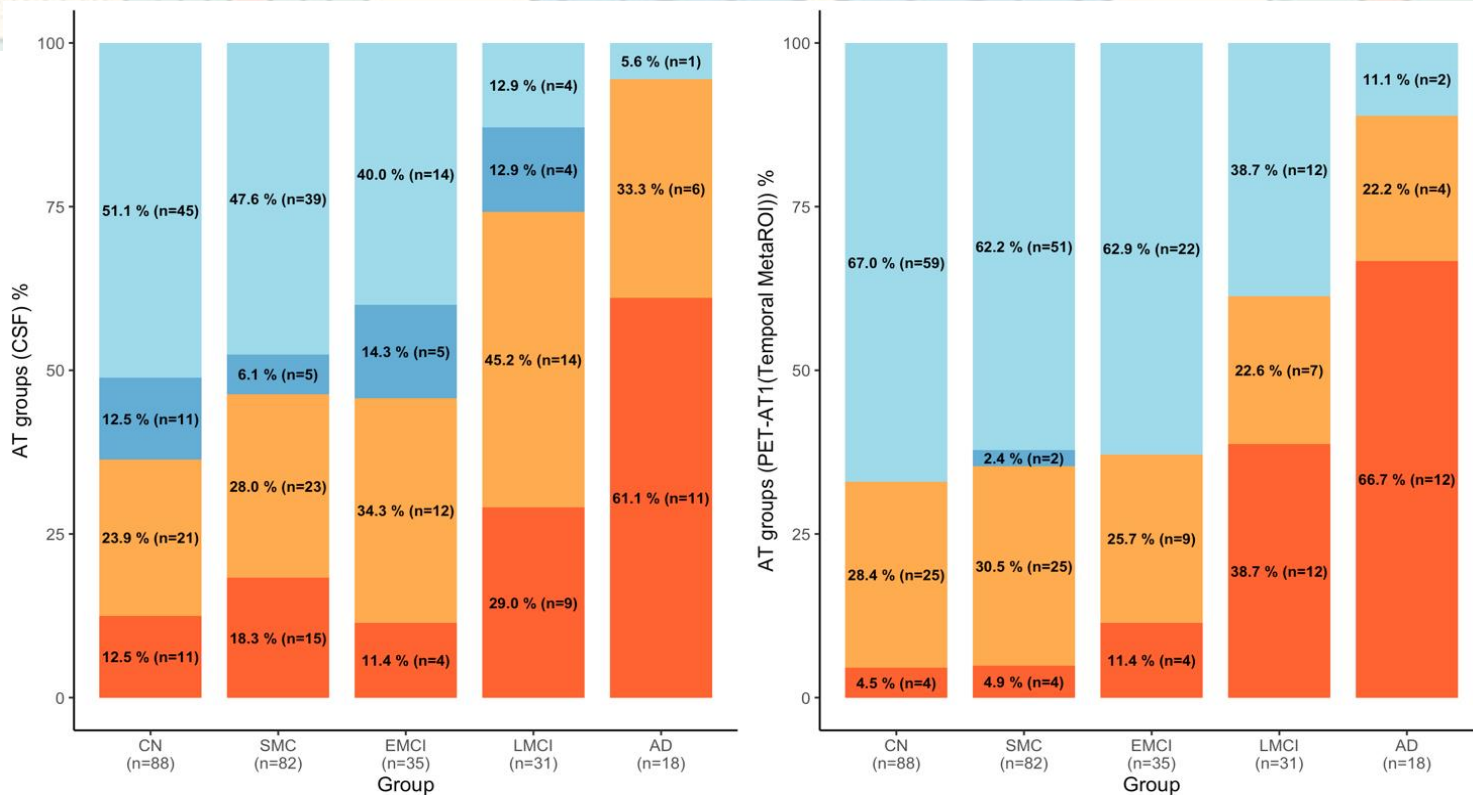
- b) to evaluate which of the investigated biomarkers proves better in predicting prospective cognitive decline.

ATN paper: General characteristics

| | CN (N=88) | SMC (N=82) | EMCI (N=35) | LMCI (N=31) | AD (N=18) | Total (N=254) | p value |
|--|-------------|-------------|--------------------------|-----------------------------|-------------------------------|---------------|----------------------|
| Age, years | | | | | | | 0.556 ¹ |
| Mean (SD) | 72.9 (7.4) | 71.3 (6.5) | 72.3 (7.8) | 73.6 (8.4) | 72.1 (9.7) | 72.3 (7.5) | |
| Range | 56.0 - 90.4 | 57.1 - 90.4 | 57.8 - 88.1 | 55.9 - 88.2 | 55.5 - 87.8 | 55.5 - 90.4 | |
| Sex | | | | | | | < 0.001 ² |
| M | 37 (42.0%) | 25 (30.5%) | 21 (60.0%) | 19 (61.3%) | 14 (77.8%) | 116 (45.7%) | |
| F | 51 (58.0%) | 57 (69.5%) | 14 (40.0%) | 12 (38.7%) | 4 (22.2%) | 138 (54.3%) | |
| Education, years | | | | | | | 0.074 ¹ |
| Mean (SD) | 17.1 (2.0) | 16.5 (2.1) | 16.3 (2.9) | 15.9 (2.4) | 16.2 (2.7) | 16.6 (2.3) | |
| Range | 12.0 - 20.0 | 12.0 - 20.0 | 12.0 - 20.0 | 10.0 - 20.0 | 12.0 - 20.0 | 10.0 - 20.0 | |
| APOE4 carrier | | | | | | | 0.040 ² |
| Missing (n) | 0 | 1 | 0 | 0 | 0 | 1 | |
| No | 61 (69.3%) | 45 (55.6%) | 25 (71.4%) | 16 (51.6%) | 7 (38.9%) | 154 (60.9%) | |
| Yes | 27 (30.7%) | 36 (44.4%) | 10 (28.6%) | 15 (48.4%) | 11 (61.1%) | 99 (39.1%) | |
| MMSE | | | | | | | < 0.001 ¹ |
| Mean (SD) | 28.9 (1.2) | 29.2 (1.0) | 28.4 (1.4) ^b | 26.9 (2.6) ^{a,b,c} | 22.3 (1.9) ^{a,b,c,d} | 28.2 (2.3) | |
| Range | 25.0 - 30.0 | 26.0 - 30.0 | 25.0 - 30.0 | 19.0 - 30.0 | 17.0 - 26.0 | 17.0 - 30.0 | |
| CDR | | | | | | | < 0.001 ¹ |
| Mean (SD) | 0.0 (0.1) | 0.0 (0.0) | 0.5 (0.1) ^{a,b} | 0.5 (0.1) ^{a,b} | 0.7 (0.3) ^{a,b,c,d} | 0.2 (0.3) | |
| Range | 0.0 - 0.5 | 0.0 - 0.0 | 0.0 - 0.5 | 0.0 - 1.0 | 0.5 - 1.0 | 0.0 - 1.0 | |
| ADNI mem. comp. score | | | | | | | < 0.001 ¹ |
| Mean (SD) | 1.1 (0.5) | 1.0 (0.5) | 0.4 (0.4) ^{a,b} | 0.1 (0.5) ^{a,b,c} | -0.8 (0.6) ^{a,b,c,d} | 0.7 (0.7) | |
| Range | -0.2 - 2.7 | -0.2 - 2.3 | -0.3 - 1.4 | -1.0 - 0.9 | -1.6 - 0.4 | -1.6 - 2.7 | |
| Follow up time interval, months | | | | | | | 0.002 ¹ |
| Missing (n) | 43 | 47 | 6 | 1 | 5 | 102 | |
| Mean (SD) | 20.2 (6.7) | 17.3 (6.3) | 17.1 (8.0) | 14.4 (5.3) ^a | 14.4 (5.1) ^a | 17.3 (6.8) | |
| Range | 0.0 - 28.2 | 10.7 - 28.4 | 3.9 - 36.6 | 4.1 - 26.3 | 10.4 - 28.2 | 0.0 - 36.6 | |

1) Linear Model ANOVA; 2) Pearson's Chi-squared test ; a,b,c,d denote significant differences respectively with CN, SMC, EMCI and LMCI with Tukey Post Hoc. p < 0.05. a.,b.,c.,d. p < 0.001

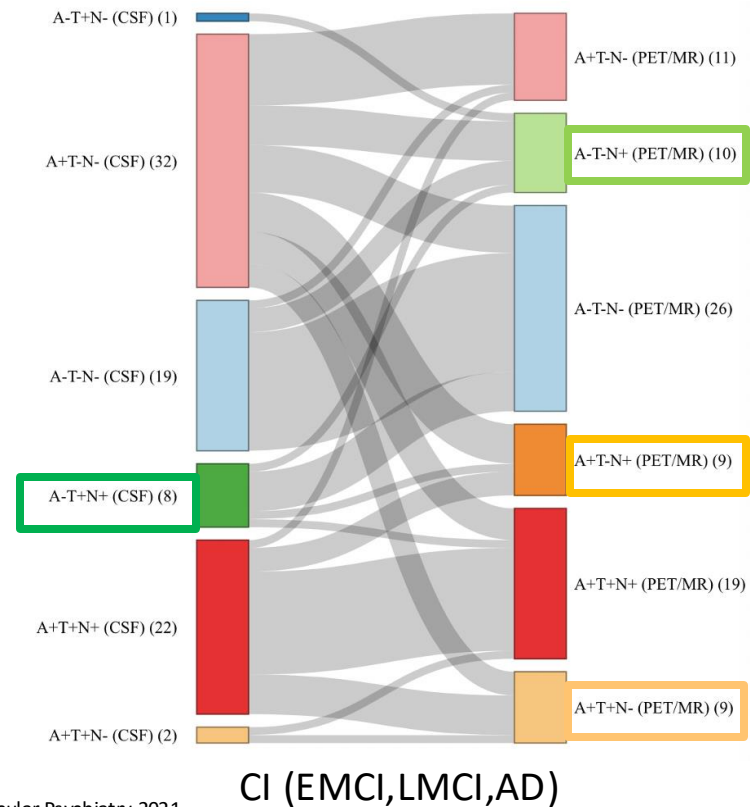
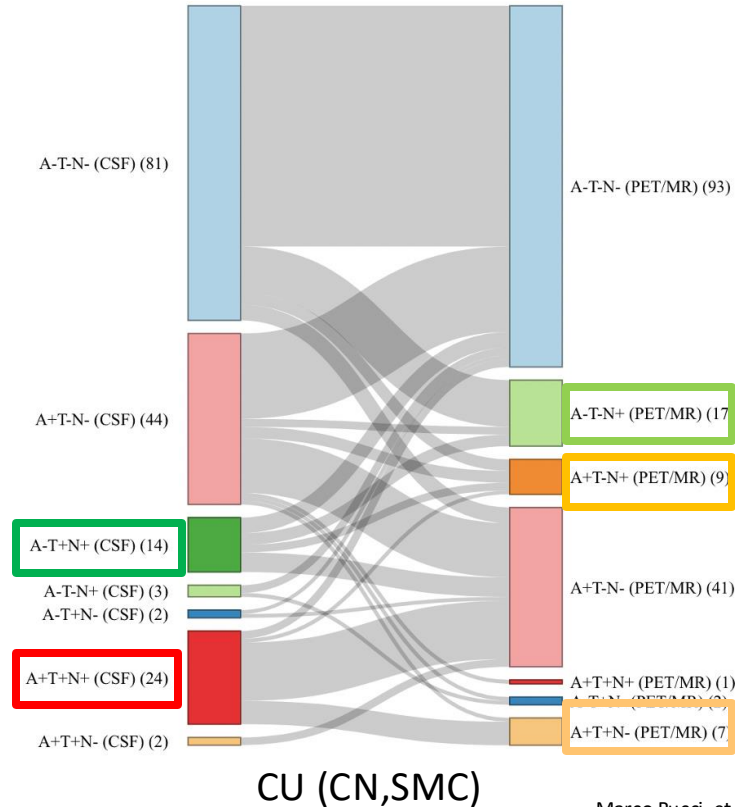
ATN paper: A/T Profiles – CSF A-T+ > PET



AT classification A-T- A-T+ A+T- A+T+

Results – AT(N) profiles

Discordance between biomarkers

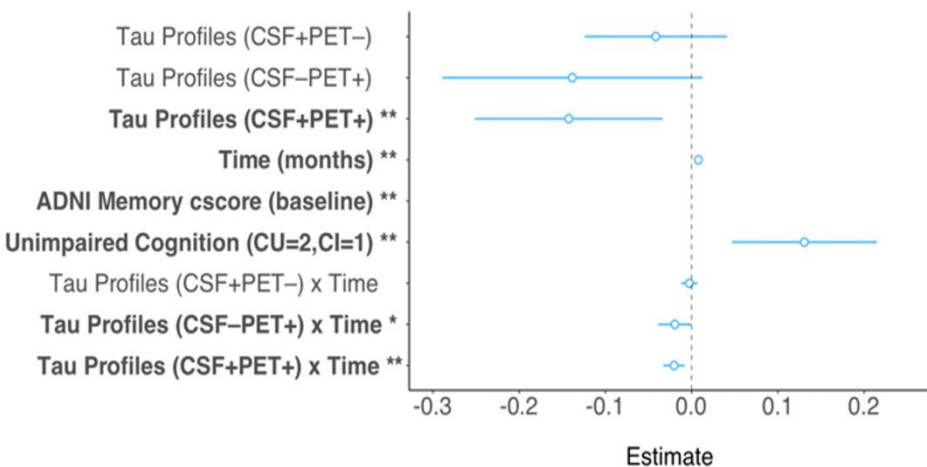




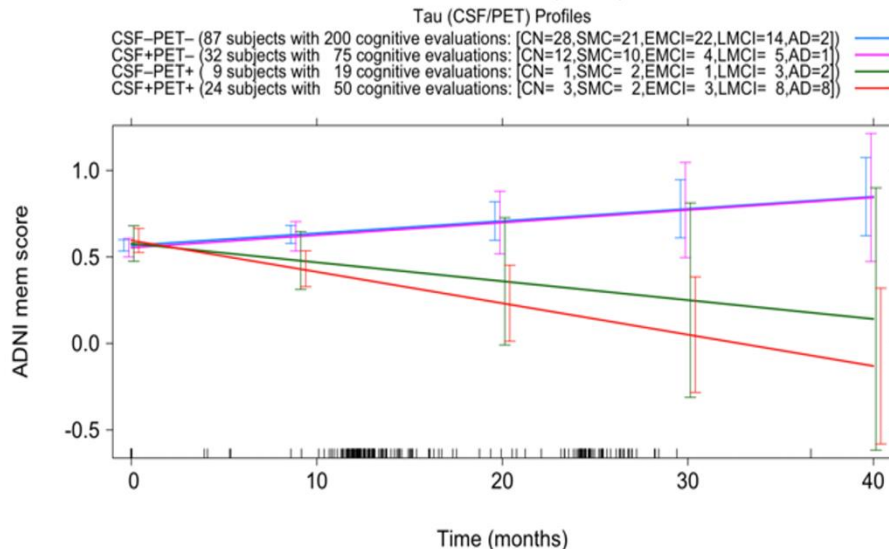
Aim 2 – Prediction of cognitive decline via LMM (Linear Mixed Models)

Results – CSF/PET Tau profiles to predict Cog. Decline: Tau PET better than CSF for prediction

Linear Mixed Model predicting (Model 6)
ADNI mem composite cognitive score



Tau CSF vs Tau PET (Temporal metaROI)
Profiles x Time - interaction effect (Model 6)



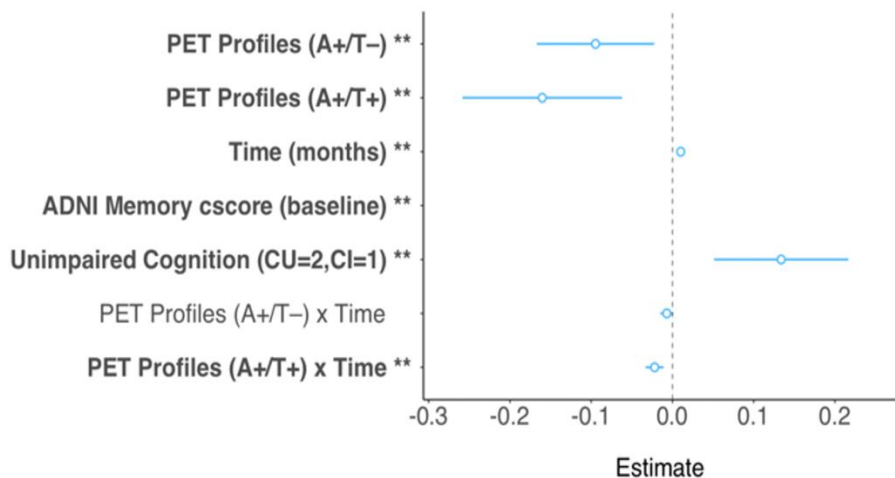
Note: Gender and ApoE4 carrier status were not significant or did not improve the model

** $p \leq 0.01$, * $p \leq 0.05$

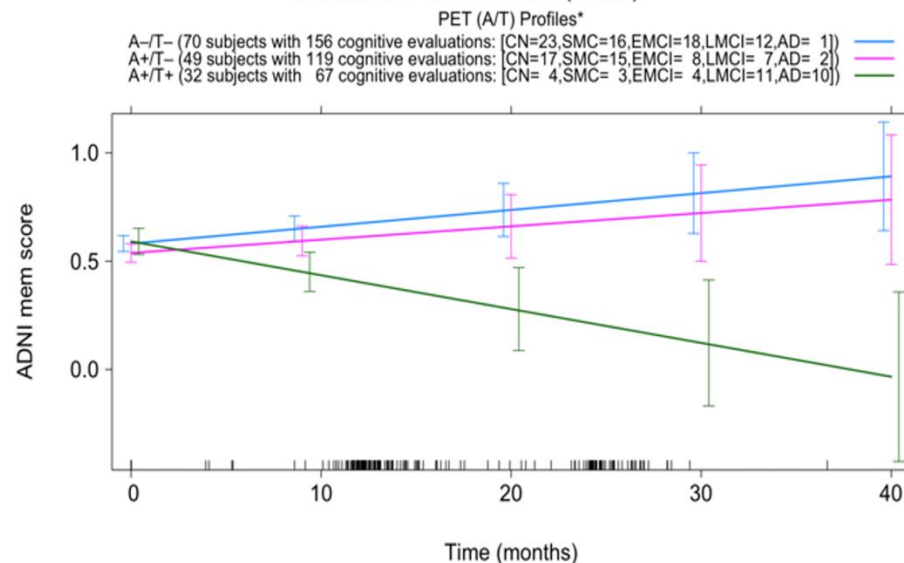
Results – A/T PET profiles to predict Cog. decline

Tau PET is a preferable predictor to Amy PET

Linear Mixed Model predicting (Model 6)
ADNI mem composite cognitive score



Amy PET vs Tau PET (Temporal metaROI)
Profiles x Time - interaction effect (Model 6)



Note: Gender and ApoE4 carrier status were not significant or did not improve the model

** $p \leq 0.01$

* PET (A-/T+) profile included only 1 subject (with borderline values) and was dropped from the analysis

Conclusions

- While biomarkers for amyloid-beta in CSF and imaging agree considerably, CSF and imaging biomarkers for tau and neurodegeneration proved not to be interchangeable.
- Tau PET positivity was superior to phosphorylated tau and amyloid- β PET in predicting a cognitive decline in the Alzheimer's disease continuum.

Background

- Plasma biomarkers have shown promising performance in research cohorts in discriminating between different stages of Alzheimer's disease (AD).
 - ↑ Plasma GFAP, in elderly individuals at high risk of AD (Chatterjee et al, 2021) and in carriers of autosomal dominant AD mutations before symptoms manifestation (Chatterjee et al, 2022).
 - Plasma pTau181 and pTau231, in autopsy studies, had the highest sensitivity and specificity in detecting AD neuropathological changes compared to pathology diagnoses (Smirnov et al, 2022).

Research cohorts tend to have strict inclusion and exclusion criteria, which lead to a higher degree of patient homogeneity, facilitating interpretability of results.

Clinical cohorts should provide valuable insights on the clinical utility of plasma biomarkers ahead of their incorporation in a real-world setting.

- Amyloid- β PET when used clinically has an added diagnostic value, especially in patients with unclear diagnosis (Leuzy et al, 2019).
 - It is of interest to investigate whether single plasma biomarkers or in combination could predict amyloid- β PET positivity (or negativity) in clinical setting.



Aims

- Evaluate plasma biomarkers in a real-world clinical setting in patients undergoing memory clinical assessment in a tertiary memory clinic:
 - Evaluate plasma biomarkers association to amyloidosis in brain (Amyloid- β PET)
 - Test if plasma biomarkers alone or in combination can predict amyloid positivity assessed as visual read of Amyloid- β PET

Methods (1)

- Tertiary memory clinic of Karolinska University Hospital
- Extensive clinical assessment
 - neuropsychological testing, CT/MRI, CSF biomarker analysis
- [18F]flutemetamol PET (A β -PET) examination
 - visual reads, quantification with Centiloids
- Blood samples taken in the same time frame for plasma biomarker analyses
 - Plasma GFAP, NFL, A β 42 and A β 40 (Quanterix, SIMOA)
 - Plasma pTau-231, pTau-181 (in-house assay kits from Gothenburg Univ.)

Methods (2) – Study population

Characteristics of the study population and diagnostic subgroups

126 patients

| | MCI A β - (N=30) | pAD (N=18) | ADD (N=51) | Non-AD (N=23) | CU (N=4) | Total (N=126) | p value |
|--------------|---------------------------|---------------|---------------|------------------|--------------|---------------|-------------|
| Age | | | | | | | 0.808 (1) |
| -- Mean (SD) | 65.87 (10.66) | 66.83 (8.41) | 64.12 (7.26) | 65.70 (8.74) | 64.00 (2.16) | 65.21 (8.47) | |
| Sex | | | | | | | 0.186 (2) |
| -- F | 17 (56.7%) | 14 (77.8%) | 28 (54.9%) | 9 (39.1%) | 2 (50.0%) | 70 (55.6%) | |
| -- M | 13 (43.3%) | 4 (22.2%) | 23 (45.1%) | 14 (60.9%) | 2 (50.0%) | 56 (44.4%) | |
| MMSE* | | | | | | | < 0.001 (1) |
| -- Mean (SD) | 25.57 (3.36) | 27.50 (1.92) | 25.38 (3.38) | 23.32 (4.04) | 29.50 (0.58) | 25.50 (3.53) | |
| Centiloid** | | | | | | | < 0.001 (1) |
| -- Mean (SD) | -1.02 (16.15) | 72.31 (23.32) | 87.95 (24.84) | -1.44 (17.28) | -7.41 (2.24) | 45.59 (47.79) | |

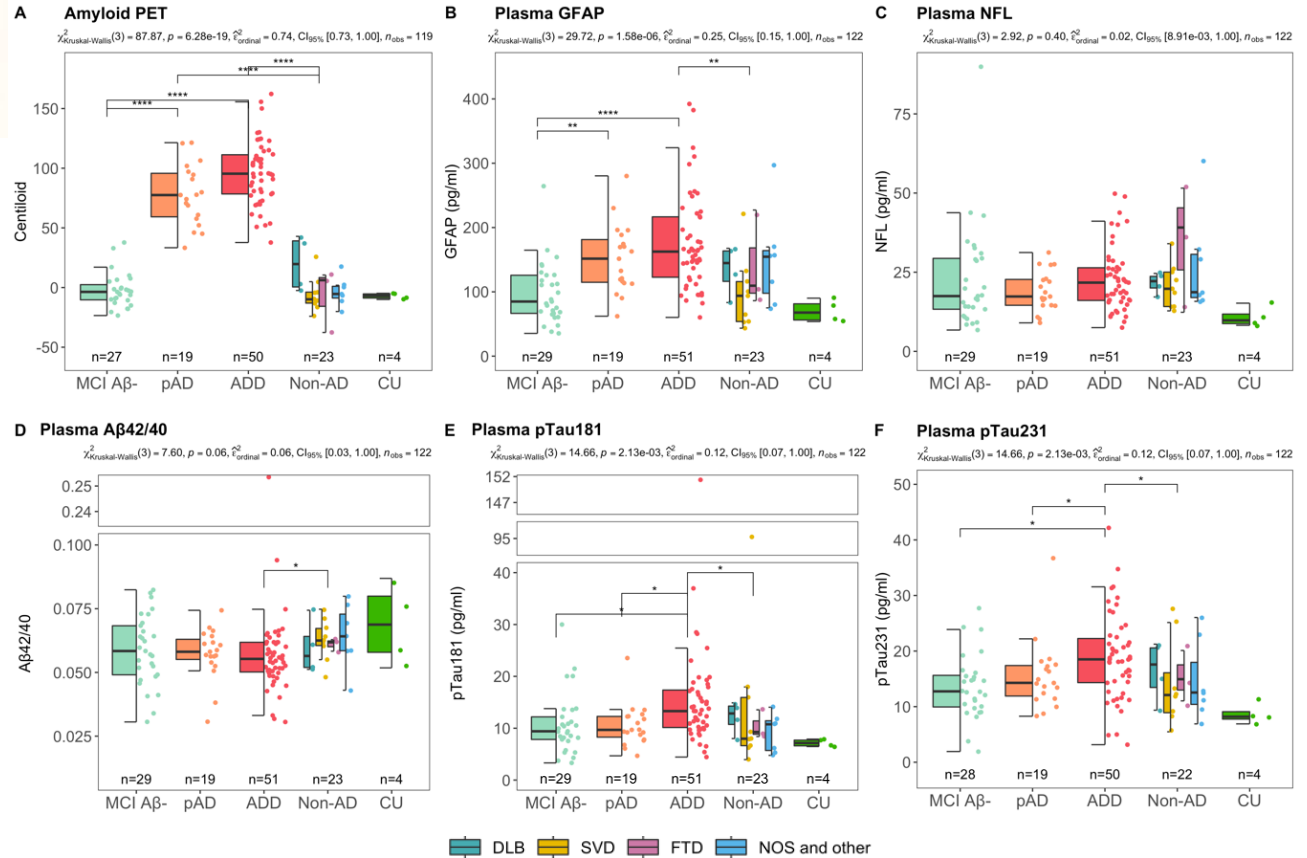
MCI, Mild Cognitive Impairment; pAD, Prodromal AD; ADD, Alzheimer's Disease Dementia; Non-AD, Non-AD dementias, CU, Cognitive Unimpaired. (1) - Kruskal-Wallis test, (2) – Pearson's χ^2 test

Methods (3) - Statistical analyses

- Group differences, tested with non-parametric tests corrected for multiple comparisons
- Correlation coefficients (Spearman's)
- ROC curves, to predict for Amyloid- β PET positivity
- LASSO regressions to combine multiple variables (and dropping the ones not contributing to the model) for prediction of Amyloid- β PET positivity (cross-validation 10-fold of the models)

Results (1)

- Plasma GFAP levels are different between MCI $A\beta$ - and prodromal AD (MCI $A\beta$ +) groups
- Plasma pTau181 and pTau231 levels were different between prodromal AD and ADD
- Plasma NFL and $A\beta$ 42/40 did not differ among AD continuum groups.



MCI, Mild Cognitive Impairment; pAD, Prodromal AD; ADD, Alzheimer's Disease Dementia; Non-AD, Non-AD dementias, CU, Cognitive Unimpaired.

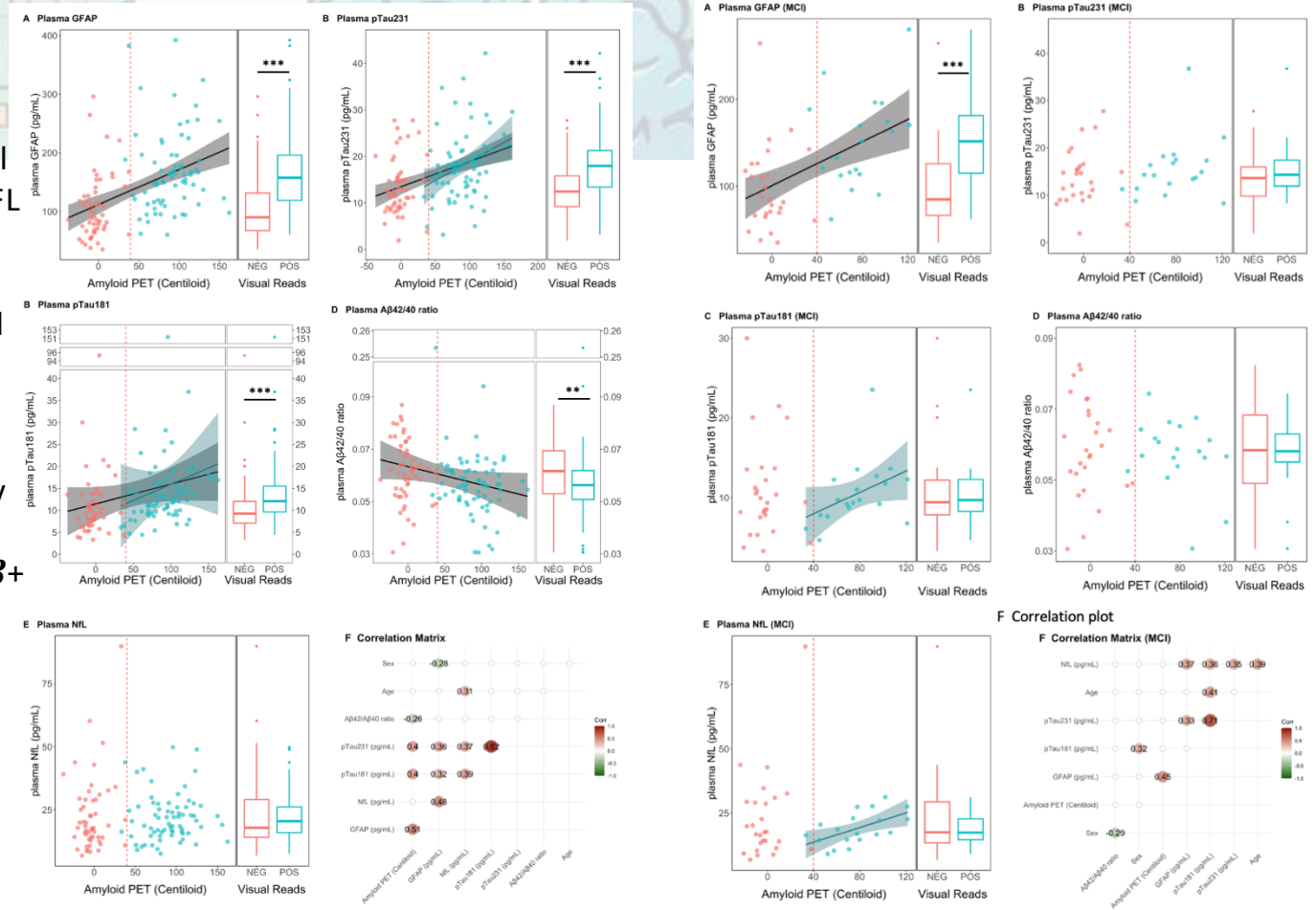
DLB, Lewy Body Dementia; SVD, Subcortical Vascular Dementia; FTD, Fronto-Temporal Dementia; NOS, Not Otherwise Specified Dementia.

Results (2)

Whole group

Mild Cognitive Impairment (MCI) group

- In the whole group all plasma BM except NFL are increased in the $A\beta+$ PET group compared to $A\beta-$ and are associated to $A\beta$ PET Centiloids.
- In the MCI group only plasma GFAP is different between $A\beta+$ and $A\beta-$ PET groups and associated with Centiloids



Results (3) In the MCI before PET group:

Plasma BMs combined has 100% Sensitivity and Negative Predictive Value.

Plasma GFAP results superior for AUC to others' biomarkers but with low specificity.

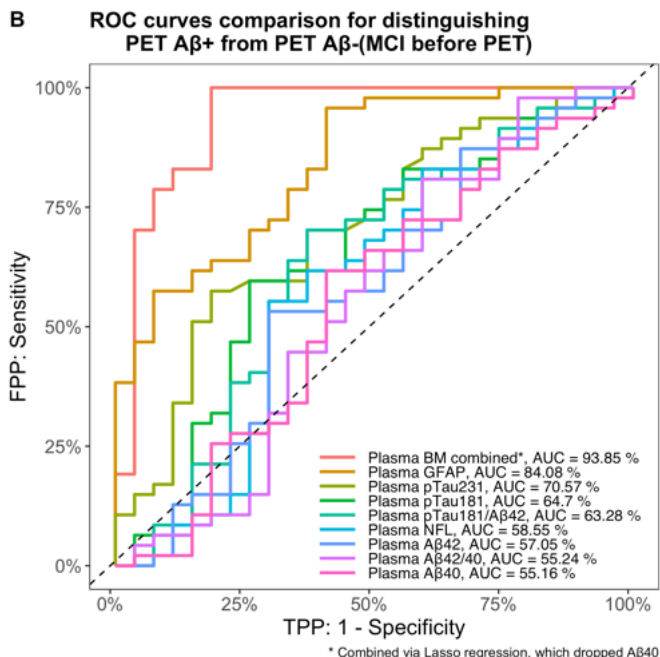


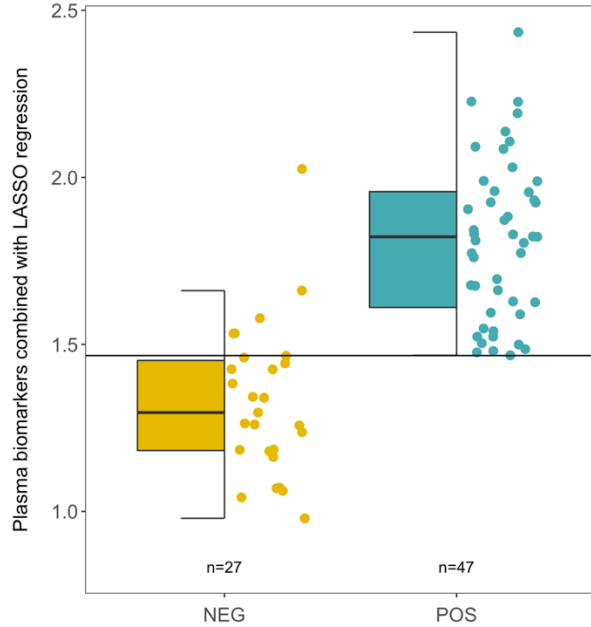
Table 2. Diagnostic performance plasma BM: MCI before PET

| Biomarker(s) | AUC (%) | Specificity (%) | Sensitivity (%) | PPV (%) | NPV (%) |
|--|---------|-----------------|-----------------|---------|---------|
| Plasma BM combined via Lasso regression (dropped Aβ40) | 93.9 | 81.5 | 100.0 | 90 | 100 |
| Plasma GFAP | 84.1 | 59.3 | 95.7 | 80 | 89 |
| Plasma pTau231 | 70.6 | 81.5 | 57.4 | 84 | 52 |
| Plasma pTau181/Aβ42 | 63.3 | 63.0 | 70.2 | 77 | 55 |
| Plasma pTau181 | 64.7 | 74.1 | 59.6 | 80 | 51 |
| Plasma Aβ42 | 57.1 | 70.4 | 53.2 | 76 | 46 |
| Plasma Aβ42/40 | 55.2 | 40.7 | 80.9 | 70 | 55 |
| Plasma Aβ40 | 55.2 | 59.3 | 61.7 | 72 | 47 |
| Plasma NFL | 58.6 | 70.4 | 55.3 | 76 | 48 |

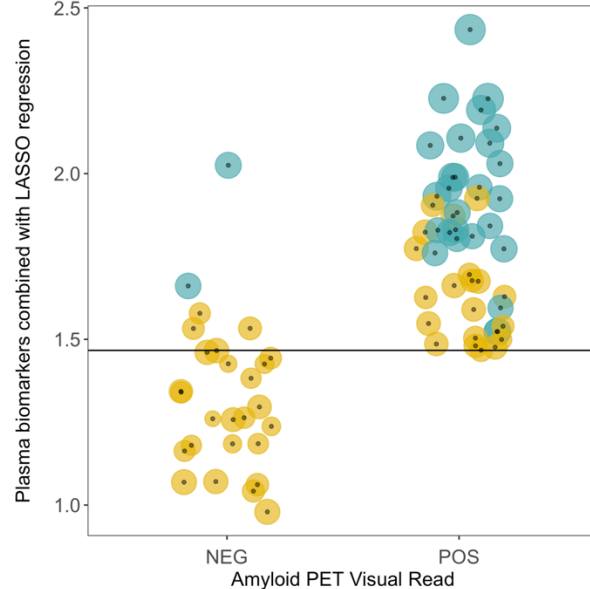
Results (4) In the MCI before PET group:

Plasma biomarkers combined results superior for AUC to others' biomarkers alone and Plasma GFAP and Plasma pTau231 are important contributors to the pooled variable.

D Plasma biomarkers predicting amyloid PET

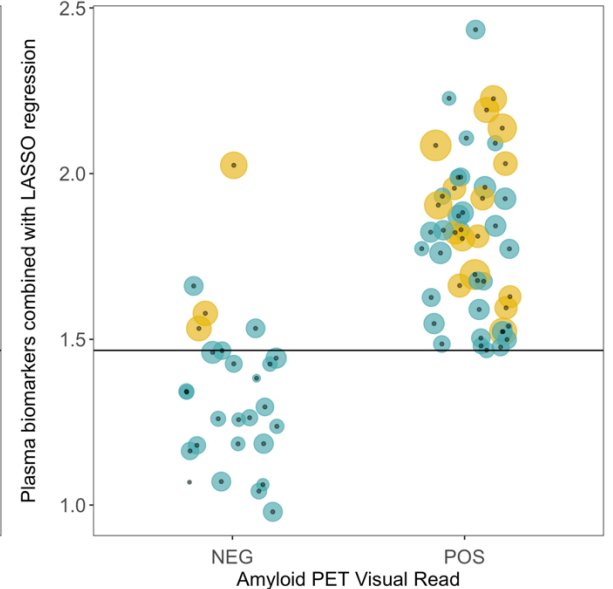


E Plasma biomarkers predicting amyloid PET (GFAP)



- Plasma GFAP < 143 (pg/mL) (cut-off for NPV maximization)
- Plasma GFAP >= 143 (pg/mL) (cut-off for NPV maximization)

F Plasma biomarkers predicting amyloid PET (pTau231)

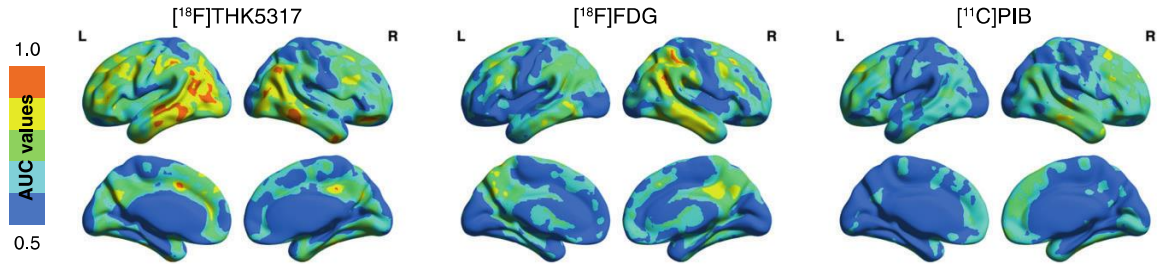


- Plasma pTau231 < 19.3 (pg/mL) (cut-off for NPV maximization)
- Plasma pTau231 >= 19.3 (pg/mL) (cut-off for NPV maximization)

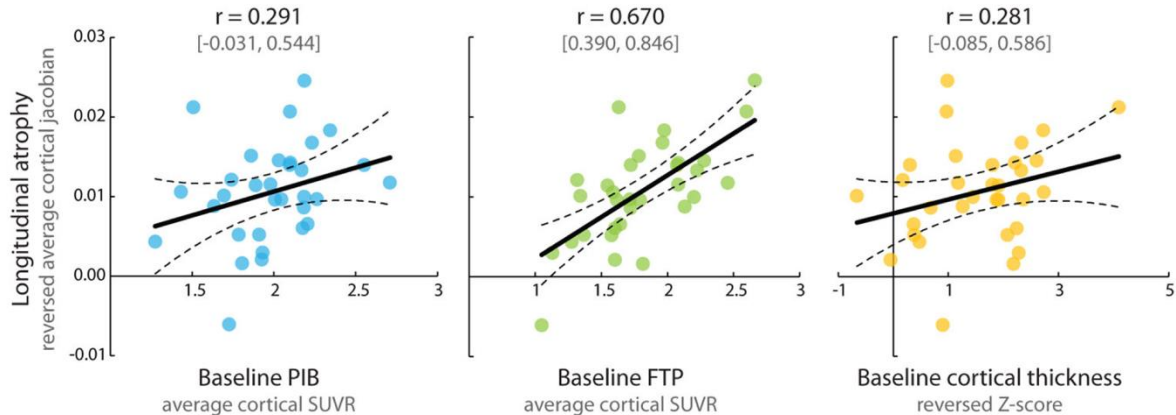
Summary and conclusions

- Plasma BM (especially GFAP) are associated to accumulation of amyloid in the brain in symptomatic clinical cases (especially in MCI)
- Plasma BMs when combined in a pooled variable (with also age and sex) resulted to have the highest negative predictive value (NPP), minimizing the amount of false negatives and being candidate for rule-out rule (if negative no $A\beta$ PET accumulation)
- More studies are needed to confirm these results and evaluate the effect on follow-up data on cognition and conversion to AD (our results on a small sub-sample indicate plasma NFL as a biomarker of interest)

Associations between PET and cognitive decline and atrophy



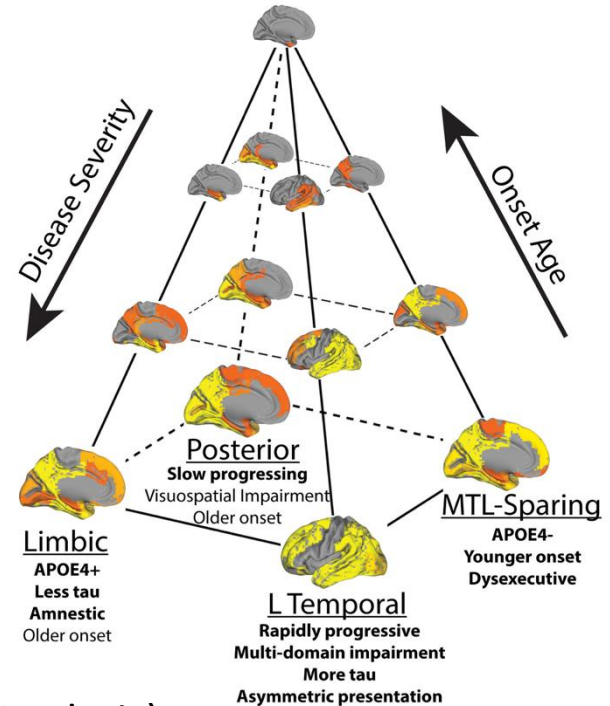
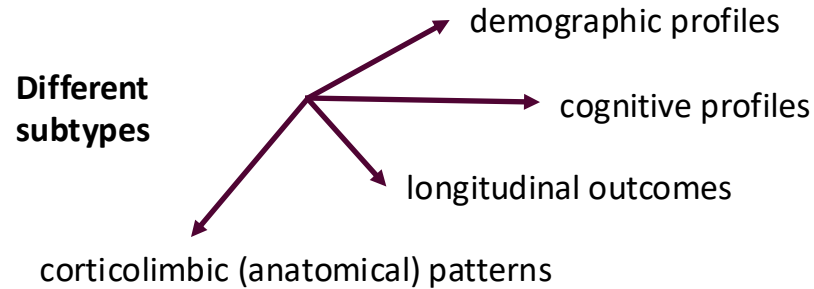
Chiotis K et al. 2020



La Joie et al. 2020

Distinct trajectories of tau deposition in AD

Variation in tau pathology is common and systematic, perhaps warranting a re-examination of the notion of “typical AD”, and a revisiting of tau pathological staging



SuStain method (Subtype and Stage Inference Model Analysis)

Brain Tau and Amyloid PET and ML: SuStAin

nature
medicine

ARTICLES

<https://doi.org/10.1038/s41591-021-01309-6>



Four distinct trajectories of tau deposition identified in Alzheimer's disease

Jacob W. Vogel¹✉, Alexandra L. Young², Neil P. Oxtoby^{3,4}, Ruben Smith^{5,6}, Rik Ossenkoppele^{5,7}, Olof T. Strandberg⁵, Renaud La Joie⁸, Leon M. Aksman^{3,9}, Michel J. Grothe^{10,11}, Yasser Iturria-Medina¹, the Alzheimer's Disease Neuroimaging Initiative^{*}, Michael J. Pontecorvo¹², Michael D. Devous¹², Gil D. Rabinovici^{8,13}, Daniel C. Alexander^{3,4}, Chul Hyung Lyoo¹⁴, Alan C. Evans¹ and Oskar Hansson^{5,15}✉

RESEARCH ARTICLE OPEN ACCESS

Spatial-Temporal Patterns of β -Amyloid Accumulation

A Subtype and Stage Inference Model Analysis

Lyduine E. Collij, PhD, Gemma Salvadó, PhD, Viktor Wottschel, PhD, Sophie E. Mastenbroek, MSc, Pierre Schoenmakers, BSc, Fiona Heeman, MSc, Leon Aksman, PhD, Alle Meije Wink, PhD, Bart N.M. Berckel, PhD, MD, Wiesje M. van de Flier, PhD, Philip Scheltens, PhD, MD, Pieter Jelle Visser, PhD, MD, Frederik Barkhof, PhD, MD, Sven Haller, PhD, MD, Juan Domingo Gispert, PhD, and Isadora Lopes Alves, PhD, for the Alzheimer's Disease Neuroimaging Initiative; for the ALFA study

Correspondence
Dr. Collij
l.collij@amsterdamumc.nl

Neurology 2022;98:e1692-e1703. doi:10.1212/WNL.000000000000200148

Amyloid PET and ML: SuStAin

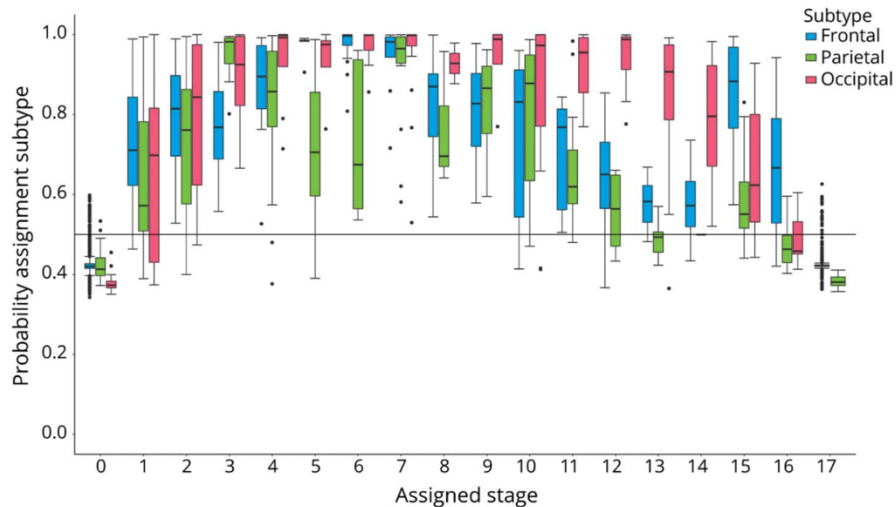
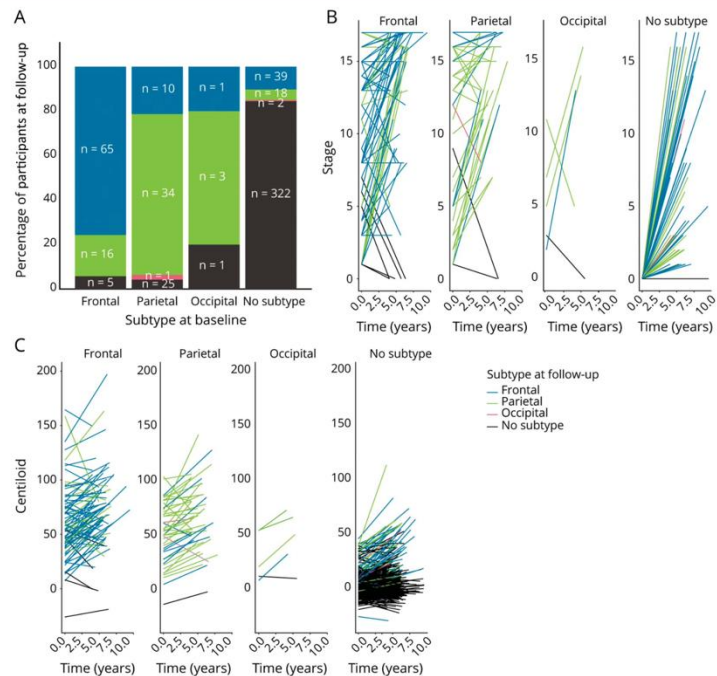


Figure 4 Longitudinal Validation



(A) Subtype assignment at baseline vs at follow-up. Spaghetti plots illustrate the change in (B) stage and (C) Centiloid units per subtype as assigned at baseline. Lines are color coded to show changes in subtype assignment at follow-up. Overall, changes in stage are associated with changes in Centiloid and yearly rates of change were lowest for the frontal subtype.

Brain Tau and Cognition: ML clustering pipeline

Fig. 2: The clustering pipeline for the definition of SDs and FDs in the case of the ADAS-Cog13 score.

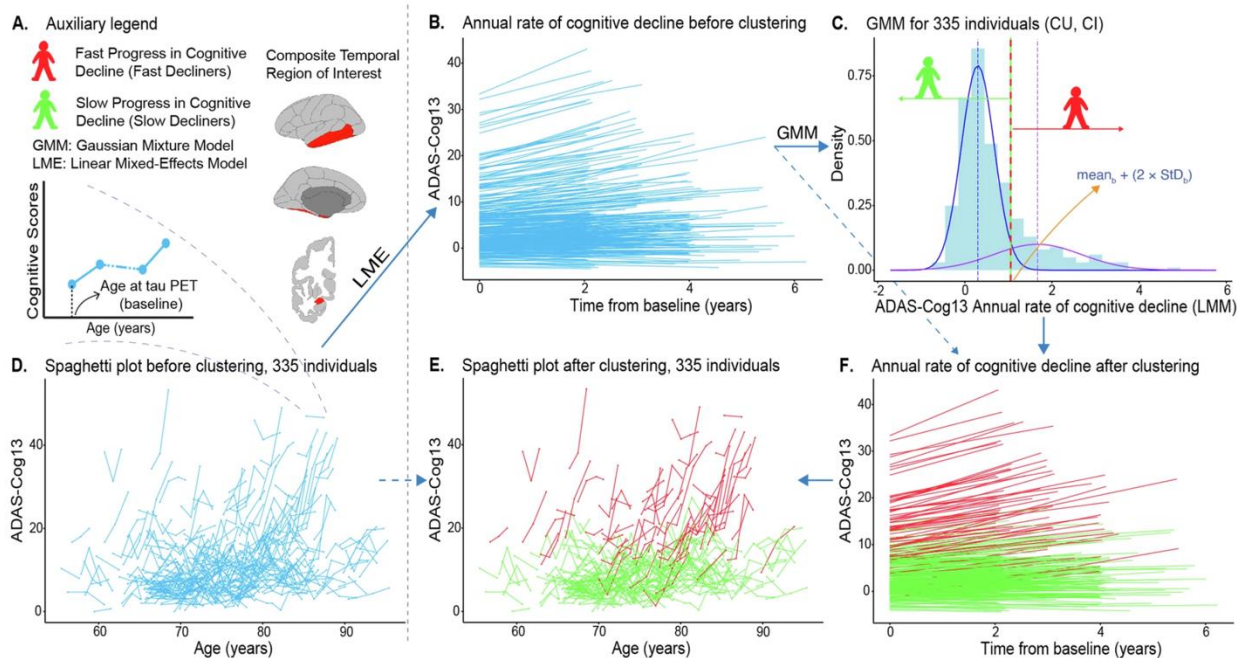
From: [Tau PET positivity predicts clinically relevant cognitive decline driven by Alzheimer's disease compared to comorbid cases; proof of concept in the ADNI study](#)

ARTICLE OPEN

Check for updates

Tau PET positivity predicts clinically relevant cognitive decline driven by Alzheimer's disease compared to comorbid cases; proof of concept in the ADNI study

Konstantinos Ioannou¹, Marco Bucci^{1,2}, Antonios Tzortzakakis^{1,4}, Irina Savitcheva⁴, Agneta Nordberg^{1,2}, Konstantinos Chiotis^{1,5,6} and for the Alzheimer's Disease Neuroimaging Initiative*



Brain Tau and Cognition

Molecular Psychiatry

www.nature.com/mp

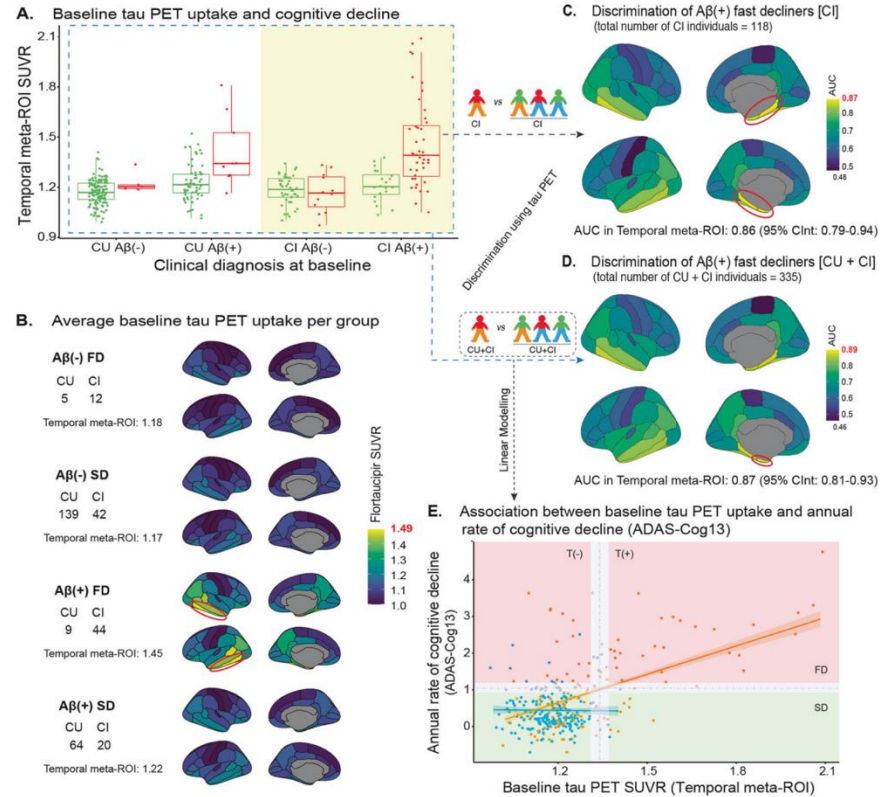
ARTICLE OPEN

Check for updates

Tau PET positivity predicts clinically relevant cognitive decline driven by Alzheimer's disease compared to comorbid cases; proof of concept in the ADNI study

Konstantinos Ioannou¹, Marco Bucci^{1,2}, Antonios Tzortzakakis^{3,4}, Irina Savitcheva⁴, Agnetta Nordberg^{1,2}, Konstantinos Chiotis^{1,5,6*} and for the Alzheimer's Disease Neuroimaging Initiative*

- Tau PET imaging showed high accuracy to predict the subset of A β (+) individuals that will show AD-relevant cognitive decline.
- Overall, tau PET can predict a population of high clinical interest and should be considered as a combined diagnostic and prognostic tool with both clinical and research applications for the management of cognitively impaired individuals.



Acknowledgements

Nordberg's Translational Molecular Imaging Lab
Prof. Agneta Nordberg, PhD, MD
Marina Bluma, PhD
Konstantinos Chiotis, PhD, MD
Irina Savitcheva, PhD, MD
Konstantinos Ioannou, MSc



Rinne Lab - ADImaging



Thanks for the attention